Measuring and Modelling Mechanochemical Reaction Kinetics

Journal:	*ChemComm*
Manuscript ID	CC-COM-04-2020-002992.R1
Article Type:	Communication

COMMUNICATION

Measuring and Modelling Mechanochemical Reaction Kinetics

Alejandro Boscoboinik,[a] Dustin Olson,[a] Heather Adams,[a,b] Nicholas Hopper,[a] and Wilfred T. Tysoe*[a]

Received 00th January 2020,
Accepted 00th January 2020

DOI: 10.1039/x0xx00000x

Quasi-static density functional theory calculations of the rate of mechanochemical decomposition of methyl thiolate species adsorbed on Cu(100) accurately reproduce the experimental normal-stress dependent rates measured in ultrahigh vacuum by an atomic force microscopy tip. This allows precise analytical models for mechanochemical reaction kinetics to be developed.

Rates of chemical reactions can be accelerated thermally, by electrons (electrochemistry) or photons (photochemistry), or by the imposition of a mechanical force (mechanochemistry). Mechanical activation is one of the oldest methods of inducing chemical reactions; there are reports from over two millennia ago of mechanochemical reduction of cinnabar to mercury.[1] More recently a wide range of organic and inorganic mechanochemical syntheses have been reported [2-6] and mechanochemical processes are ubiquitous in biology.[7-9] The most economically important example of mechanochemistry is the reaction of lubricant additives that form friction- or wear-reducing films, known as tribochemistry,[10] which has recently been shown to be mechanochemically induced.[11-13]

Mechanochemical reactions are stress-induced processes in which the shape of the Born-Oppenheimer potential energy surface is modified by an external force to reduce the energy barrier between metastable minima, where the transition over the modified energy barrier is thermally assisted and thus depends on temperature. Mechanochemical kinetics are often described by the Bell model,[14] where the rate constant for the reaction in the absence of an external force k_0 is given by $k_0 = Aexp\left(-\frac{E_{act}}{k_BT}\right)$, where E_{act} is the activation energy, k_B is the Boltzmann constant and T the absolute temperature. An external force F modifies the energy profile by a potential given by $-Fx$. To first order, this provides a simple equation for the reaction rate constant $k(F) = k_0exp\left(\frac{F\Delta x^\ddagger}{k_BT}\right)$. $\Delta x^\ddagger$ is referred to as the activation length, defined as a distance from the initial to the transition state. Since experiments generally measure the contact stress σ (force per unit area), the Bell model is often written as $k(\sigma) = k_0exp\left(\frac{\sigma\Delta V^\ddagger}{k_BT}\right)$, where $\Delta V^\ddagger$ is an activation volume, the activation length multiplied by the area over which the applied stress acts.

Similar concepts of the way in which energy landscapes are modified by an external force were first used by Prandtl [15] to model crystal plasticity, and by Eyring to model energy dissipation during fluid shear (its viscosity).[16] It was subsequently used to explain a wide range of stress-induced phenomena [17] such as material fracture,[18] rubber friction,[19] and atomic-scale friction and wear;[20, 21] mechanically induced processes are ubiquitous in chemistry, physics and materials science.

Exponential stress dependences of mechanochemical reaction rates have been found experimentally,[11, 12, 22-25] leading to measured values of the activation volume of ~10 Å^3. However, the activation volume of a mechanochemical reaction cannot generally be predicted *a priori*. This occurs for a number of reasons. Neither the nature of the elementary steps in the reaction pathways nor the direction of the force with respect to the energy landscape are generally known for the systems that have been studied hitherto.[26] This lack of a theoretical framework with which to analyze and ultimately predict the rates of tribo/mechanochemical reactions has impeded the growth of the field of mechanochemistry and the development of novel lubricants or the design of new mechanochemical syntheses. As a result, the subfield of mechanochemistry is significantly less well developed than other fields of chemistry.

The experimental issues are addressed by accurately measuring the normal-stress induced decomposition kinetics of methyl thiolate (CH_3–$S_{(ads)}$) overlayers on Cu(100) by an atomic force microscope (AFM) tip in ultrahigh vacuum (UHV) (See Figure S1). This reaction has been implicated as a crucial step in the gas-phase lubrication of copper by dimethyl disulphide (DMDS).[27-29]

---

[a] *Department of Chemistry and Biochemistry and Laboratory for Surface Studies*
University of Wisconsin-Milwaukee
Milwaukee, WI 53211, USA
E-mail: wtt@uwm.edu.
[b] *Dr. H. Adams*
Present address: Alcami Corporation
Germantown, WI 53022, USA.

Electronic Supplementary Information (ESI) available: Experimental Procedures; Indentation Profiles, Reaction Rates and Pressure Distribution; Measurement of Reaction Rates and Activation Energies; Control Experiments; Figures S1 to S12. See DOI: 10.1039/x0xx00000x

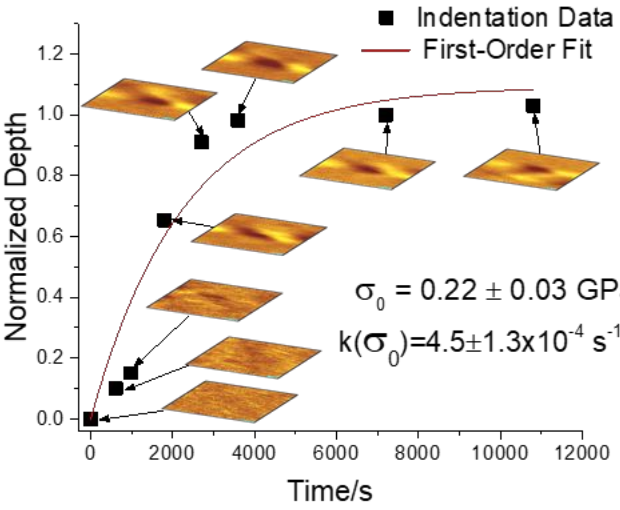

Fig. 1: Typical indentation kinetics of the mechanochemical decomposition of methyl thiolate on Cu(100). The extent of reaction was gauged from the maximum indention depths at the centre of the contact, which were measured at a normal load F_N of 118 nN for various times by imaging the indent using 0.1 µm × 0.1 µm topographic contact-mode AFM scans at a nonperturbative load. Images (30 nm × 30 nm scan area) of the indented region are shown on the figure.

While molecular dynamics (MD) simulations are used to theoretically analyze mechanochemical reactions,[24, 30] and reactive potentials are available for the S–C–Cu system,[31] the small time steps required to carry out MD calculations generally necessitate the use of sliding speeds and temperatures that are much higher than those of the experiment. We take advantage of the large disparity between the time scales of the AFM tip compared to the rapid motion of the adsorbed molecular species to calculate the rate of normal-stress-induced methyl thiolate decomposition on copper using density functional theory (DFT) under quasi-static conditions.[32] This is similar to the COnstrained Geometries for simulating External Force (COGEF) method,[33] and analogous to the Born-Oppenheimer approximation for molecules.[34]

Mechanochemical reactions have also been explained in terms of the influence of an external force on the molecular electronic structure.[35] However, the orbital and the geometrical explanations are really identical because changes in molecular geometry caused by an external stress induce a shift in the molecular energy levels that can lower the reaction activation energy. Such changes in electronic structure are just those that occur as the reaction proceeds from the initial to the transition state and are essentially two ways of describing the same phenomenon.

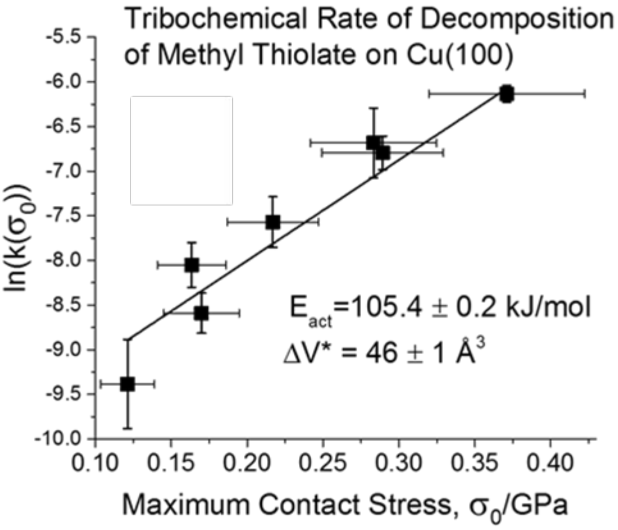

Fig. 2: Rates of normal-contact-stress induced mechanochemical decomposition of methyl thiolate species on Cu(100) showing a plot of $ln\ (k(\sigma_0))$, where k is the rate constant for the mechanochemical decomposition of methyl thiolate overlayer on Cu(100) at 298 K measured from the maximum depth at the center of the indentation, as a function of the maximum contact stress, σ_0. The linear dependence demonstrates that the mechanochemical decomposition rates obey the Bell model.[14] The intercept yields an activation energy for methyl thiolate decomposition in the absence of a normal stress of 105.4 ± 0.2 kJ/mol when using a pre-exponential factor of $1\times10^{14}\ s^{-1}$, in excellent agreement with experimental measurements [37] and theoretical calculations.[38,39]

Finally, we note that methyl thiolate decomposition (Fig. S1) is an ideal reaction for studying mechanochemical kinetics because methyl thiolate is thermally stable on copper to ~430 K, but undergoes shear-induced decomposition at room temperature. The activation energy measured for methyl thiolate decomposition is ~100 kJ/mol,[36] and is in good agreement with the results of DFT calculations. The reaction rate measured from the yield of the gas-phase reaction products formed during rubbing *in vacuo* is first-order in methyl thiolate coverage.[37] Crucially, DFT calculations reveal that adsorbed methyl thiolate species decompose by the methyl group both translating laterally and moving vertically downwards; the reaction coordinate has a component perpendicular to the Cu(100) surface. This predicts that a normal stress alone should lower the activation barrier for methyl thiolate decomposition and thus accelerate the reaction.

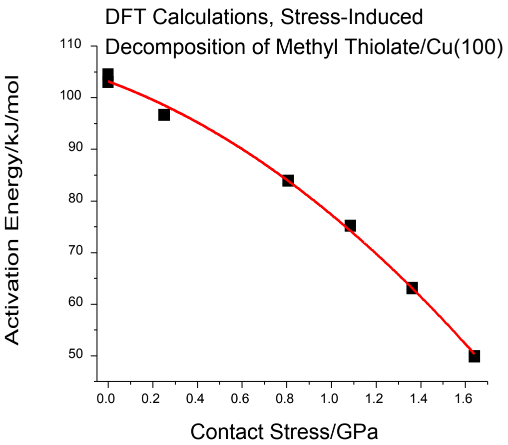

Fig. 3: Plot of the activation energy calculated by DFT as a function of contact stress for the normal-stress-induced mechanochemical decomposition of methyl thiolate species adsorbed on Cu(100).

We carry out single-asperity compression experiments on methyl thiolate overlayers formed by dosing DMDS on Cu(100) at room temperature (298 K) in a UHV AFM with normal loads F_N from 40 to 118 nN for reaction times up to ~6.3×10^4 s. The mechanochemical decomposition of a methyl thiolate overlayer creates indentations that are imaged using contact- mode AFM at non-perturbing loads, where it was observed that the maximum depth increases with contact (reaction) time (Fig. 1). Because the elastic contact pressure varies with position within the contact,[38] the extent of reaction was measured from the depth at the center of the indentation where the contact stress is a maximum, and the observed shape of the indent is in agreement with this assumption (Fig. S5). The depth initially increases as a function of time and eventually saturates, indicating the completion of the mechanochemical reaction. The time dependence of the extent of reaction obeys first-order kinetics with respect to methyl thiolate coverage over the whole coverage range (Figs. 1 and S6). This kinetic order is in agreement with previous measurements of methyl thiolate decomposition rates obtained from the yield of gas-phase products for microscale sliding on copper in UHV. [37, 39,29] Fits to the data yield first-order rate constants $k(F_N)$. The contact areas were estimated from the widths of the indentations d after completion of the reactions (Fig. S5),[22] and the maximum normal stresses exerted at the center of the contact were calculated from: $\sigma_0 = 6F_N/\pi d^2$.

A linear plot of $\ln(k(\sigma_0))$ versus σ_0 is shown in Fig. 2 confirming that the reaction rate does vary exponentially with contact stress, consistent with the Bell model.[14] Extrapolation to zero stress yields an activation energy of 105.4 ± 0.2 kJ/mol, in agreement with experimental measurements of the activation energy of methyl thiolate decomposition on copper.[36] The slope of the plot in Fig. 2 yields an activation volume $\Delta V^\ddagger$ = 46 ± 1 Å^3, similar to values measured previously for mechanochemical reactions on surfaces.[11, 12, 22-25]

Quasi-static DFT calculations were carried out by compressing by a clean Cu(100) counterface slab against a methyl-thiolate covered slab, where the energies and configurations were calculated for different values of slab separation (Fig. S4, Movie S1). The results (Fig. S9) reveal an initial slightly attractive interaction as the slabs approach, consistent with the snap into contact as the tip approaches the surface (Fig. S3), but the interaction becomes repulsive as the slabs move closer together. The repulsive part of the potential varies parabolically with distance enabling the normal contact stresses to be calculated. Nudged-elastic band (NEB) calculations of the energy barriers (Fig. S10) reveal a decrease in activation energy with increasing normal stress (Fig. 3). Note that the calculated activation energy for zero applied stress is in excellent agreement with the experimental value.[36]

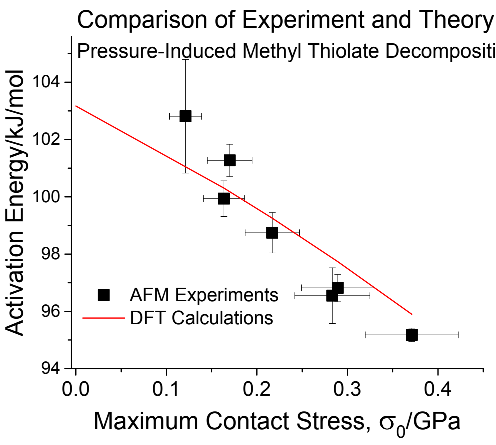

Fig. 4: : The experimental data are shown plotted directly as reaction activation energy versus maximum contact stress, compared with the results of DFT calculations (——).

The results of the calculations are compared to experiment in Fig. 4 (——). Note that the experimentally accessible normal stress range is lower than that used for the quantum calculations and thus reflects only the initial, almost linear portion of the second-order curve shown in Fig. 3. These results indicate that quasi-static DFT calculations accurately predict stress-induced activation energies. The transition-state energy decreases linearly with normal force (Fig. S11), with an effective activation length $\Delta z^\ddagger$ of 0.31 ± 0.03 Å. Combining the stress-dependent initial- and final-state energies, an analytical expression for the stress-dependent activation energy can be obtained as: $E_{act}(\sigma) = E^0_{act} - \sigma\Delta z^\ddagger - (1/2k)\sigma^2$, and is fitted to the calculations in Fig. 3. Note that such second-order behavior is predicted by an extended-Bell model [40] and the curvature observed in Fig. 3 is known as the anti-Hammond effect.[41]

It is commonly found that the activation energies for elementary reaction steps on metal surfaces scale with the heats of reaction [42] so that $E_{act} = E^0_{act} + \alpha E_r$, known as the Evans-Polanyi relation.[43] The stress-dependent activation energy also scales linearly with the heat of reaction (Fig. S12), with α = 0.95 ± 0.02 and is similar to values found for bond dissociation reactions on metals.[42].

In summary, precise measurements of the mechanochemical reaction kinetics of the normal-stress induced decomposition of a well-defined model system consisting of a methyl thiolate overlayer on a Cu(100) single crystal substrate reveal that the reaction rate increases exponentially with normal stress, with an activation volume of

46 ± 1 Å^3 and an activation energy in the limit of zero stress that is in good agreement with that for the thermal reaction

In order to understand the decomposition kinetics of methyl thiolate species on Cu(100), the variation in activation energy as a function of applied stress was modelled using quasi-static first principles DFT calculations. Adsorption geometries and energies of methyl thiolate were calculated for various normal stresses and the corresponding activation energies were obtained using the NEB method, yielding results that are in excellent agreement with experiment.

DFT calculations reveal that the final state is also stabilized by the normal stress, where the stress-dependent activation energy varies linearly with the overall heat of reaction and thus obeys the Evans-Polanyi relation. Such linear free energy relationships have been very useful in analyzing catalytic reaction pathways [44-47] and are likely to be similarly useful for describing mechanically induced reactions.

Importantly, the ability to predict mechanochemical reaction kinetics using quasi-static DFT calculations will set the stage for studying mechanical activation for stresses that do not necessarily coincide with the lowest-energy pathway, as well as for studying more complex mechanochemical systems. This will aid in further developing robust theories for mechanochemical activation and for ultimately predicting mechanochemical activity. For example, the next stage is to study the combined effects of normal and lateral stresses on mechanochemical reaction rates. In the case of the decomposition of methyl thiolate species on Cu(100), the rate is expected to depend strongly on how colinear the sliding direction is with respect to the reaction coordinate of the lowest-energy pathway.

Finally, the availability of simple, but precise models for calculating the variation in reaction activation energy with applied stress will allow the velocity and temperature dependences of mechanochemical reaction rates to be predicted using a similar approach to that in the Prandtl-Tomlinson model for frictional energy dissipation.[15, 17, 20, 48]

Conflicts of interest

There are no conflicts to declare.

Notes and references

1. H. J. Theophrastus, *Theophrastus's history of stones : with an English version, and critical and philosophical notes, including the modern history of the gems, &c., described by that author, and of many other of the native fossils*, London, 1774.
2. A.-S. Duwez, S. Cuenot, C. Jerome, S. Gabriel, R. Jerome, S. Rapino and F. Zerbetto, *Nature Nanotechnology*, 2006, **1**, 122-125.
3. M. Konôpka, R. Turanský, J. Reichert, H. Fuchs, D. Marx and I. Štich, *Physical Review Letters*, 2008, **100**, 115503.
4. S. L. Craig, *Nature*, 2012, **487**, 176-177.
5. S. L. James, C. J. Adams, C. Bolm, D. Braga, P. Collier, T. Friscic, F. Grepioni, K. D. M. Harris, G. Hyett, W. Jones, A. Krebs, J. Mack, L. Maini, A. G. Orpen, I. P. Parkin, W. C. Shearouse, J. W. Steed and D. C. Waddell, *Chemical Society Reviews*, 2012, **41**, 413-447.
6. J. Ribas-Arino and D. Marx, *Chemical Reviews*, 2012, **112**, 5412-5487.
7. Carlos Bustamante, Yann R. Chemla, Nancy R. Forde and D. Izhaky, *Annual Review of Biochemistry*, 2004, **73**, 705-748.
8. J. N. Brantley, C. B. Bailey, K. M. Wiggins, A. T. Keatinge-Clay and C. W. Bielawski, *Polymer Chemistry*, 2013, **4**, 3916-3928.
9. K. Sriram, Justin G. Laughlin, P. Rangamani and Daniel M. Tartakovsky, *Biophysical Journal*, 2016, **111**, 208-221.
10. T. Mang and W. Dresel, *Lubricants and lubrications*, Wiley-VCH, Weinheim; New York; Chichester, 2001.
11. J. Zhang and H. Spikes, *Tribology Letters*, 2016, **63**, 1-15.
12. N. N. Gosvami, J. A. Bares, F. Mangolini, A. R. Konicek, D. G. Yablon and R. W. Carpick, *Science*, 2015, **348**, 102-106.
13. A. Akchurin and R. Bosman, *Tribology Letters*, 2017, **65**, 59.
14. G. Bell, *Science*, 1978, **200**, 618-627.
15. L. Prandtl, *Zeitschrift für Angewandte Mathematik und Mechanik*, 1928, **8**, 85.
16. W. Kauzmann and H. Eyring, *Journal of the American Chemical Society*, 1940, **62**, 3113-3125.
17. H. Spikes and W. Tysoe, *Tribology Letters*, 2015, **59**, 1-14.
18. S. N. Zhurkov, *International Journal of Fracture Mechanics*, 1965, **1**, 11.
19. A. Schallamach, *Proceedings of the Physical Society. Section B*, 1953, **66**, 386.
20. G. A. Tomlinson, Philosophical Magazine, 1929, **7**, 905.
21. E. Gnecco, R. Bennewitz, A. Socoliuc and E. Meyer, *Wear*, 2003, **254**, 859-862.
22. J. R. Felts, A. J. Oyer, S. C. Hernández, K. E. Whitener Jr, J. T. Robinson, S. G. Walton and P. E. Sheehan, *Nature Communications*, 2015, **6**.
23. S. Raghuraman, M. B. Elinski, J. D. Batteas and J. R. Felts, *Nano Letters*, 2017, **17**, 2111-2117.
24. J. Yeon, X. He, A. Martini and S. H. Kim, *ACS Applied Materials & Interfaces*, 2017, **9**, 3142-3148.
25. L. Chen, J. Wen, P. Zhang, B. Yu, C. Chen, T. Ma, X. Lu, S. H. Kim and L. Qian, *Nature Communications*, 2018, **9**, 1542.
26. D. E. Makarov, *The Journal of Chemical Physics*, 2016, **144**, 030901.
27. O. J. Furlong, B. P. Miller, P. Kotvis and W. T. Tysoe, *ACS Applied Materials & Interfaces*, 2011, **3**, 795-800.
28. B. Miller, O. Furlong and W. Tysoe, *Tribology Letters*, 2013, **49**, 39-46.
29. H. Adams, B. P. Miller, O. J. Furlong, M. Fantauzzi, G. Navarra, A. Rossi, Y. Xu, P. V. Kotvis and W. T. Tysoe, *ACS Applied Materials & Interfaces*, 2017, **9**, 26531-26538.
30. T. Kuwahara, P. A. Romero, S. Makowski, V. Weihnacht, G. Moras and M. Moseler, *Nature Communications*, 2019, **10**, 151.
31. J. Yeon, H. L. Adams, C. E. Junkermeier, A. C. T. van Duin, W. T. Tysoe and A. Martini, *The Journal of Physical Chemistry B*, 2018, **122**, 888-896.
32. B. Chen, R. Hoffmann and R. Cammi, *Angewandte Chemie International Edition*, 2017, **56**, 11126-11142.
33. M. K. Beyer, *The Journal of Chemical Physics*, 2000, **112**, 7307-7312.
34. M. Born and R. Oppenheimer, *Annalen der Physik*, 1927, **389**, 457-484.
35. J. J. Gilman, *Science*, 1996, **274**, 65.
36. O. J. Furlong, B. P. Miller, Z. Li, J. Walker, L. Burkholder and W. T. Tysoe, *Langmuir*, 2010, **26**, 16375-16380.
37. H. L. Adams, M. T. Garvey, U. S. Ramasamy, Z. Ye, A. Martini and W. T. Tysoe, *The Journal of Physical Chemistry C*, 2015, **119**, 7115-7123.
38. K. L. Johnson, *Contact mechanics. Cambridge University Press: Cambridge; New York, 1985*.
39. H. Adams, B. P. Miller, P. V. Kotvis, O. J. Furlong, A. Martini and W. T. Tysoe, *Tribology Letters*, 2016, **62**, 1-9.
40. S. S. M. Konda, J. N. Brantley, C. W. Bielawski and D. E. Makarov, *The Journal of Chemical Physics*, 2011, **135**, 164103-164108.
41. S. M. Avdoshenko and D. E. Makarov, *The Journal of Physical Chemistry B*, 2016, **120**, 1537-1545.
42. A. Michaelides, Z. P. Liu, C. J. Zhang, A. Alavi, D. A. King and P. Hu, *Journal of the American Chemical Society*, 2003, **125**, 3704-3705.
43. M. G. Evans and M. Polanyi, *Transactions of the Faraday Society*, 1935, **31**, 875-894.
44. A. Logadottir, T. H. Rod, J. K. Nørskov, B. Hammer, S. Dahl and C. J. H. Jacobsen, *Journal of Catalysis*, 2001, **197**, 229-231.
45. T. Bligaard, J. K. Nørskov, S. Dahl, J. Matthiesen, C. H. Christensen and J. Sehested, *Journal of Catalysis*, 2004, **224**, 206-217.
46. R. A. v. Santen, M. Neurock and S. G. Shetty, *Chemical Reviews*, 2009, **110**, 2005-2048.
47. D. Loffreda, F. Delbecq, F. Vigné and P. Sautet, *Angewandte Chemie International Edition*, 2009, **48**, 8978-8980.
48. W. Tysoe, *Tribology Letters*, 2017, **65**, 48.

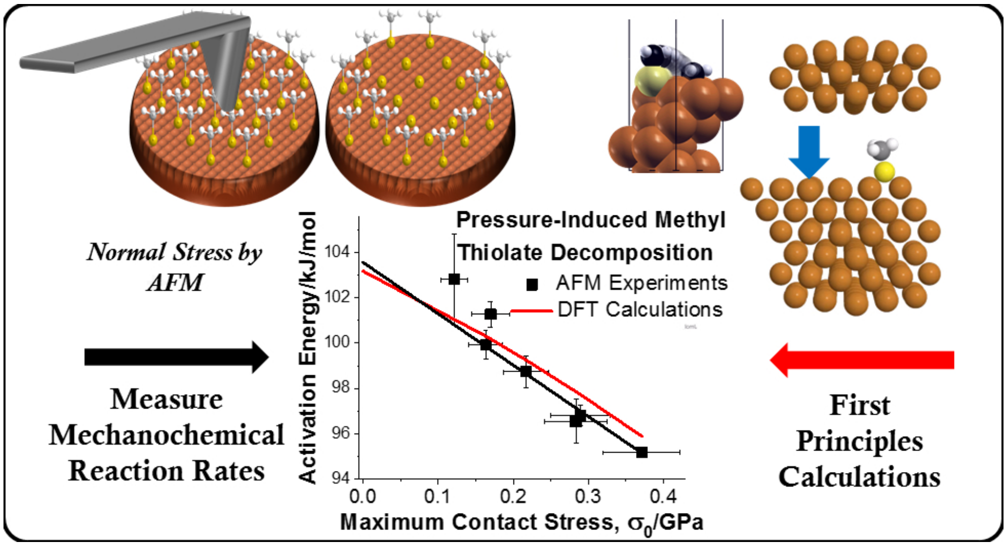

82x44mm (300 x 300 DPI)